Electronic Supplementary Material

Activated Carbon templated synthesis of a Hierarchical Zeolite Y encapsulated Iron catalyst for Enhanced Gasoline selectivity in CO-hydrogenation

Heyang Liu[a], Yajie Fu [a], Mingquan Li [a], Jiayuan Wang[a], Aqsa Noreen [a], Xinhua Gao[c], Ruiqin Yang[a], Cederick Cyril Amoo[a,b]*, Chuang Xing[a]*

[a]School of Biological and Chemical Engineering, Zhejiang University of Science and Technology, Hangzhou 310023, China

[b]Dalian National Laboratory for Clean Energy**,** Dalian Institute of Chemical Physics, Chinese Academy of Sciences, Dalian 116023, China

[c] State Key Laboratory of High-efficiency Utilization of Coal and Green Chemical Engineering, Ningxia University, Yinchuan 750021, China

*Corresponding authors.

E-mail addresses:

cedecy@dicp.ac.cn

xing@zust.edu.cn

Experimental Section

Catalyst Characterization

The metal loadings in the catalysts were determined by inductively coupled plasma-atomic emission spectroscopy (ICP-AES, Agilent 725ES). Transmission Electron Microscopy (TEM) and subsequent elemental mappings images were achieved on FEI Talos 200F at 200kV. Scanning Electron Microscopy (SEM) images of all catalysts were obtained on a SU1510. X-ray diffractions (XRD) were attained with a Rigaku Ultima IV having Cu Kα radiation foundation (4°/min at 40 kV and 20 mA). The textural properties of the samples were measured by N_2-physisorption on an Autosorb-iQ instrument (Quantachrome Co., Ltd.). A mass of 0.2 g for each sample was used in this process. The samples were initially degassed at 300 °C for 3 h to remove unwanted organics, gases, and water. The surface area was calculated from the Brunauer-Emmett-Teller (BET) equation and pore volume from the single-point method. H_2- temperature-programmed reduction (H_2-TPR) of all catalysts were performed on the BELCAT-B3 instrument, equipped with a thermal conductivity detector (TCD). The samples were initially pretreated in inert N_2 at a flow rate of 30 mL min^{-1} and a temperature of 300 °C. Afterward, the equipment was cooled, and gas with H_2/Ar = 10/90 at a flow rate of 20 mL min^{-1} was introduced as the temperature was raised from 100 to 700 °C, at a heating rate of 10 °C min^{-1}. NH_3 temperature-programmed desorption (NH_3-TPD) of the samples was also carried out on a BELCAT-B3 instrument equipped with a TCD. The samples were first pretreated in pure N_2 at a flow rate and a temperature of 30 mL min^{-1} and 300 °C, respectively. Thereafter, the equipment was cooled, and gas with NH_3/He = 5/95 at a flow rate of 20 mL min^{-1} was introduced as the temperature was raised from 100 to 700 °C. H_2/CO TPD measurements were performed using a BELCAT-B3 unit equipped with a thermal conductivity detector (TCD). The catalysts (0.2 g) were reduced in H_2 flow (40 ml·min^{-1}) at 400 °C for 4 h and then cooled to 50 °C. The samples were then purged with N_2 to remove weakly adsorbed species. H_2 or CO was then introduced until saturation. Afterward, the samples were heated under He flow at a heating rate of 10 °C/min^{-1}, while the TCD detector was used to detect the desorbed H_2 or CO. Pyridine FTIR was achieved on an FTIR-650 FT-IR spectrometer to qualitatively analyze the acidity on the catalysts. The samples were prepared on a thin wafer and pre-treated at 450 °C in a vacuum. The prepared slides were then cooled down to room temperature, exposed to pyridine for 5 mins and then

finally evacuated at 150 and 350 ◦C for 30 min. Thermal analysis (TG-DSC) was achieved with a Netzsch STA449F3.

FTS reaction evaluation

FTS performances of all catalysts used in the experiment were operated in a single fixed-bed reactor under 260 °C, H_2/CO=2/1, and W/F=10 g·h/mol. For each catalyst, a mass of 0.3 g mixed with 0.5 g of quarts was loaded in a continuous flow stainless steel reactor having an inner diameter of 6.8 mm and reduced at 400 °C for 4 h in H_2 flow (40 mL/min). Two online gas chromatographs (TCD and FID) were used to analyze the effluent gaseous products. TCD and FID were equipped with an Agilent HP-Plot/Q column and a TDX-01 column respectively. Liquid products were collected in an ice trap and analyzed offline by a gas chromatograph (GC-2014, FID, Shimadzu) equipped with an Sh-Rtx-5 column.

Catalyst activity and product selectivity were calculated on a molar basis using the following formulae:

$$CO\ conversion(\%) = \frac{F_{CO_{(in)}} - F_{CO_{(out)}}}{F_{CO_{(in)}}} \times 100 \qquad (1)$$

Where; $F_{CO_{(in)}}$ *= inlet CO molar flow*

$F_{CO_{(out)}}$ *= outlet CO molar flow*

$$Hydrocarbons\ Selectivity\ (\%) = \frac{nF_{Cn\ (out)}}{F_{CO_{(in)}} - F_{CO_{(out)}}} \times 100 \qquad (2)$$

Where; C_n *= carbon number of product*

$F_{Cn\ (out)}$ *= outlet molar flowrate of product* C_n

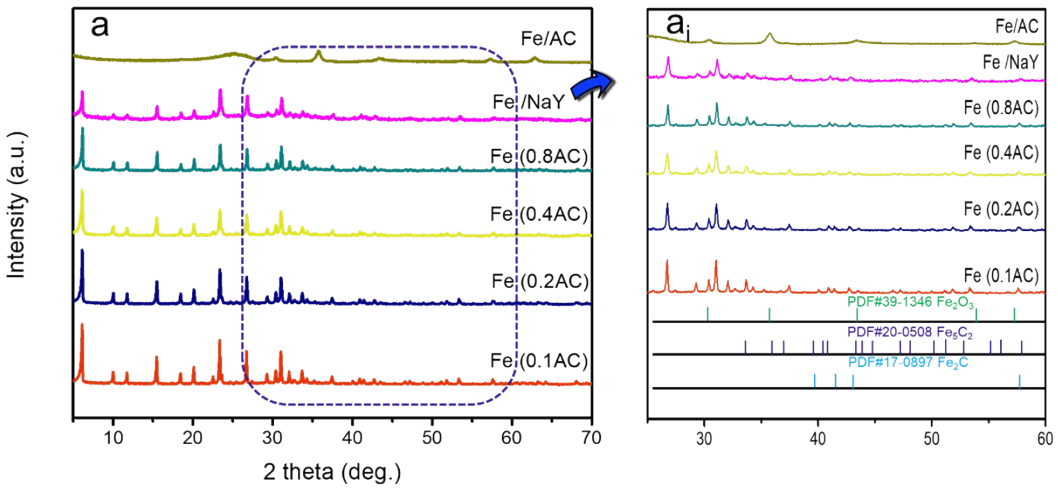

Figure S1. XRD diffractograms of all as prepared catalysts

Table S1 Properties of As-prepared catalysts.

Sample	Relative Crystallinity[a]	Fe Loading/%		Fe_2O_3 particle size/nm[d]
		I[b]	II[c]	
NaY	100	N/A	N/A	N/A
Fe(0.1AC)	84	10	10.56	5.27
Fe(0.2AC)	93	10	10.50	4.48
Fe(0.4AC)	81	10	10.42	7.65
Fe(0.8AC)	69	10	11.02	6.42
Fe/NaY	60	10	10.89	18.40
Fe/AC	N/A	10	9.4	15.60

[a]Zeolite Relative crystallinity calculated using XRD,
[b]Theoritically calculated Fe loading
[c]Fe loading obtained via ICP-AES,
[d]Average Particle Size calculated using Scherrer formula

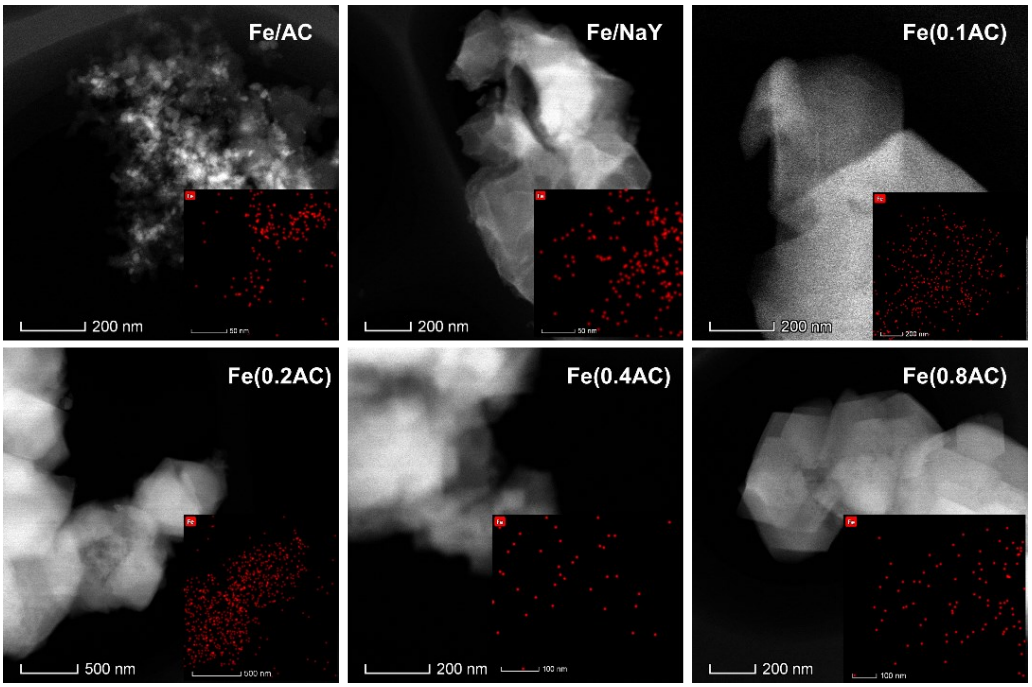

Figure S2 STEM-HAADF images of the as-prepared catalysts with associated Fe-EDX mapping

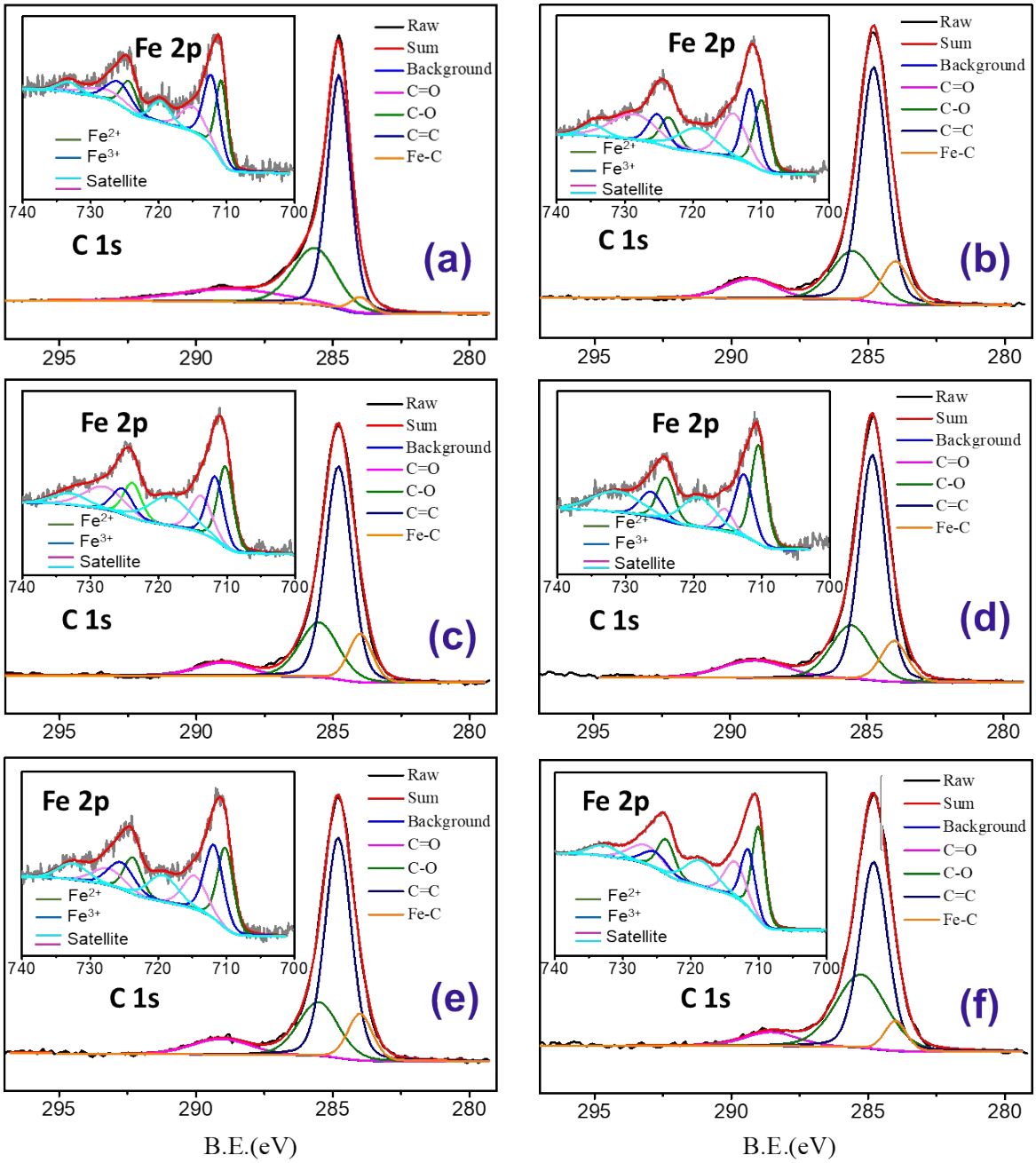

Figure S3 XPS spectra in the Fe2p and C 1s region for as-prepared (a) Fe/AC, (b) Fe(0.1), (c) Fe(0.2), (d) Fe(0.4), (e) Fe(0.8), and (f) Fe/NaY

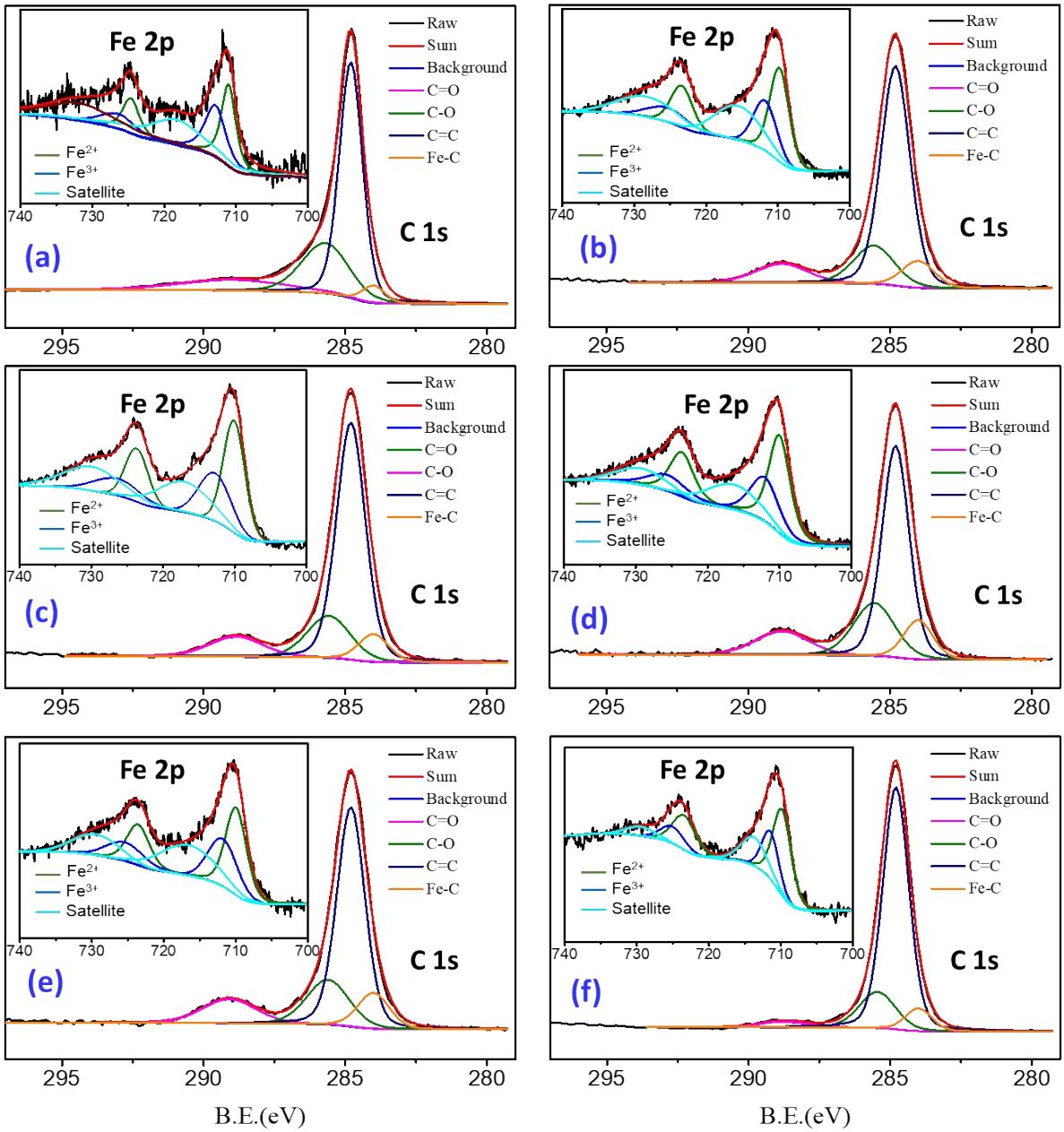

Figure S4 XPS spectra in the Fe2p and C 1s region for spent (a) Fe/AC, (b) Fe(0.1), (c) Fe(0.2), (d) Fe(0.4), (e) Fe(0.8), and (f) Fe/NaY

Table S2 Comparison of the hydrocarbon selectivity

Catalysts	Temp.(°C)	CO Conv. (%)	Selectivity(%)			ReF
			CH_4	C_2-C_4	C_{5+}	
Fe/CNTs	260	2.8	80.1	7.1	2.8	[1]
CoFe (10/5 ratio)	260	10	35	21.0	41	[2]
FeZnNa@0.6-NaZSM-5	340	27.2	10.1	36.2	52.6	[3]
FeNa@C	340	95.8	17.5	12.5	49.8	[4]
Fe/SBA-15@HZSM-5	300	57.6	15.3	220	62.7	[5]
Fe/NaY	300	52.2	28.5	25.5	46.0	[6]
Fe(0.1AC)	260	12.3	9.8	20.8	69.0	This work
Fe(0.2AC)	260	40.1	13.3	20.6	65.1	This work

References;

1. Gholami, Z.; Zabidi, N. A. M.; Gholami, F.; Vakili, M., Synthesis and characterization of niobium-promoted cobalt/iron catalysts supported on carbon nanotubes for the hydrogenation of carbon monoxide. *Journal of Fuel Chemistry and Technology* **2016,** *44* (7), 815-821.
2. de la Peña O'Shea, V. A.; Álvarez-Galván, M. C.; Campos-Martín, J. M.; Fierro, J. L. G., Fischer–Tropsch synthesis on mono- and bimetallic Co and Fe catalysts in fixed-bed and slurry reactors. *Appl. Catal., A* **2007,** *326* (1), 65-73.
3. Zhao, B.; Zhai, P.; Wang, P.; Li, J.; Li, T.; Peng, M.; Zhao, M.; Hu, G.; Yang, Y.; Li, Y.-W.; Zhang, Q.; Fan, W.; Ma, D., Direct Transformation of Syngas to Aromatics over Na-Zn-Fe5C2 and Hierarchical HZSM-5 Tandem Catalysts. *Chem* **2017,** *3* (2), 323-333.
4. Ma, G.; Xu, Y.; Wang, J.; Bai, J.; Du, Y.; Zhang, J.; Ding, M., An Na-modified Fe@C core–shell catalyst for the enhanced production of gasoline-range hydrocarbons via Fischer–Tropsch synthesis. *RSC Advances* **2020,** *10* (18), 10723-10730.
5. Xing, C.; Sun, J.; Chen, Q.; Yang, G.; Muranaka, N.; Lu, P.; Shen, W.; Zhu, P.; Wei, Q.; Li, J.; Mao, J.; Yang, R.; Tsubaki, N., Tunable isoparaffin and olefin yields in Fischer–Tropsch synthesis achieved by a novel iron-based micro-capsule catalyst. *Catalysis Today* **2015,** *251*, 41-46.
6. Amoo, C. C.; Li, M.; Noreen, A.; Fu, Y.; Maturura, E.; Du, C.; Yang, R.; Gao, X.; Xing, C.; Tsubaki, N., Fabricating Fe Nanoparticles Embedded in Zeolite Y Microcrystals as Active Catalysts for Fischer–Tropsch Synthesis. *ACS Applied Nano Materials* **2020,** *3* (8), 8096-8103.